JOC Article
pubs.acs.org/joc

Structure−Chiroptical Properties Relationship of Carbapenams by Experiment and Theory

Magdalena Woźnica, Marek Masnyk, Sebastian Stecko, Adam Mames, Bartłomiej Furman, Marek Chmielewski, and Jadwiga Frelek*

Institute of Organic Chemistry of the Polish Academy of Sciences, Kasprzaka 44/52, 01-224 Warsaw, Poland

frelek@icho.edu.pl

Received July 21, 2010

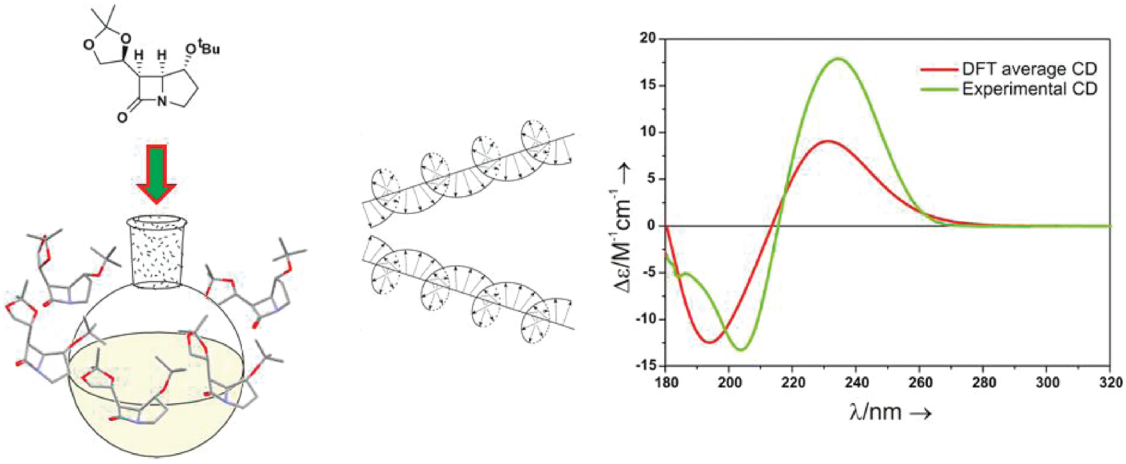

The present work examines the relationship between the molecular structure and chiroptical properties of carbapenams through use of electronic circular dichroism spectroscopy (ECD). The applicability of the helicity rule that correlates the molecular structures of various β-lactam analogues and their ECD spectra is examined against a set of differently substituted carbapenams. It is demonstrated that the studied compounds conform to the rule. The rule can be also applied to the carbapenams with an additional chromophoric unit interfering with the amide chromophore. For the representative carbapenams, the experimental curves are compared to the ECD spectra computed using time-dependent density functional theory (TDDFT) in order to validate the experimental data. The study reveals a high effectiveness of the ECD spectroscopy for the configurational assignment at the bridgehead carbon atom and demonstrates a strong dependence of the molecular conformation on substitution of the five-membered ring and side-chain flexibility of investigated carbapenams.

1. Introduction

As a part of our ongoing studies on chiroptical properties of β-lactam antibiotic analogues, we have recently published results on the structure−chiroptical properties relationship of clavams.[1] The study confirmed that the helicity rule, originally developed for oxa- and carbaanalogues of cephams,[2] is also applicable to clavams. This means that by application of the simple helicity rule assignment of the absolute configuration of the carbon atom at the ring junction in newly synthesized or isolated clavams can be done with confidence. The positive or negative sign of an electronic circular dichroism (ECD) band appearing at around 240 nm correlates with the (5*R*) or (5*S*) absolute configuration, respectively, in accordance with both the rule and the TDDFT calculations.

In the present work, we intend to test the applicability of the helicity rule to carbapenams defined as carbaanalogues

(1) Chmielewski, M.; Cierpucha, M.; Kowalska, P.; Kwit, M.; Frelek, J. *Chirality* **2008**, *20*, 621–627.

(2) (a) Łysek, R.; Borsuk, K.; Chmielewski, M.; Kałuża, Z.; Urbańczyk-Lipkowska, Z.; Klimek, A.; Frelek, J. *J. Org. Chem.* **2002**, *67*, 1472–1479. (b) Frelek, J.; Kowalska, P.; Masnyk, M.; Kazimierski, A.; Korda, A.; Woźnica, M.; Chmielewski, M.; Furche, F. *Chem.—Eur. J.* **2007**, *13*, 6732–6744. (c) Frelek, J.; Łysek, R.; Borsuk, K.; Jagodziński, J.; Furman, B.; Klimek, A.; Chmielewski, M. *Enantiomer* **2002**, *7*, 107–114.

DOI: 10.1021/jo101429k Published on Web 09/27/2010

CHART 1

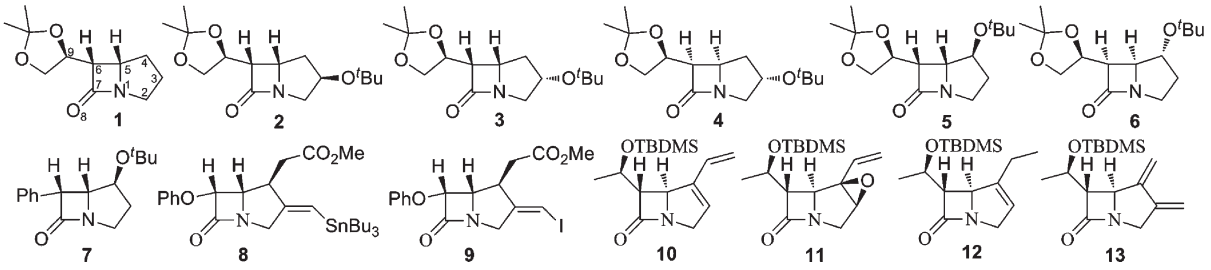

of penicillins. Carbaanalogues of penicillins and cephalosporins represent a relatively new class of antimicrobial agents with a great potential for therapeutic use owing to the broad spectrum of activity and stability toward serine β-lactamases. The clinical use of the first naturally produced antibiotic belonging to the group of carbapenems called thienamycin was successfully launched in 1979.[3] This fact initiated an interest in the clinical use of this group of compounds. However, because of the lack of stability of thienamycin in aqueous solution, a number of more stable derivatives of thienamycin were introduced for medicinal use over several years. Among them imipenem,[4] meropenem,[5] ertapenem,[5,6] and doripenem[5] were introduced to the market. Various synthetic methods are used for the preparation of thienamycin and derivatives.[7] In most of these methods, the optically pure 3-(1-hydroxyethyl)-4-acetoxy-2-azetidinone is used[8] as one of the starting materials. Since enantiomers differ in their biological properties, the knowledge of the absolute stereochemistry is essential in the quest for structural improvements leading to new bioactive compounds and attracts the attention of many synthetic chemists. This knowledge may be also appealing to pharmaceutical and biological chemists. Thus, access to methods allowing determination of the absolute stereostructure in a simple and unambiguous way is highly desirable. Since circular dichroism spectroscopy proved to be extremely useful and effective in our previous studies on azetidinones and their polycyclic derivatives,[9] we also decided to apply the same methodology in present studies. First, we want to test the validity of the aforementioned helicity rule to carbapenams. Second, we intend to examine the influence of substituents, including strongly absorbing ones, on the diagnostic ECD band. Such a substitution may substantially perturb the electronic structure of the system and therefore significantly influence the ECD spectra. In addition, the type and location of substituents can considerably affect the conformation of the five-membered ring. For example, it was demonstrated that the biological activity of penicillins is strongly dependent upon the conformation of the thiazolidine ring.[10] Therefore, the influence of conformational flexibility of the system on ECD spectra should be taken into account. Consequently, we decided to examine the impact of substituents on the conformational preferences and stability of the 4-carba-4-dethia penicillin analogues and to estimate the substituent effect on their chiroptical properties. A variety of differently substituted carbapenams presented in Chart 1 have been chosen as model compounds for this study.

To validate the helicity rule in context of the carbapenams and their substituted analogues, we decided to find a theoretical model that correlates the observed spectrum to the three-dimensional molecular structure. For this purpose, we intend to apply a combined treatment of the ECD spectroscopy and the time-dependent density functional theory. Since the ECD spectroscopy is very sensitive to minute changes in geometry and electronic structure of investigated molecules the combination of experimental and theoretical analysis will allow to draw a more definite conclusions within the scope of present research.

2. Results and Discussion

2a. Synthesis. The synthetic route used for the preparation of carbapenams **1**−**7** via the Kinugasa cycloaddition/rearrangement cascade process[11] between terminal cooper acetylides and nonracemic cyclic nitrones (shown in Scheme 1) was previously reported by our group.[12] The detailed synthetic procedure and spectral characterization, including absolute configuration determination, of compounds **1**−**7** is also included there.

SCHEME 1

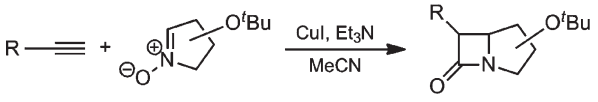

Compounds **8** and **9** were synthesized following the literature procedure presented in Scheme 2 starting from chiral azetidinone **i**.[13] In this synthesis, the key step was the free radical cyclization reaction.

(3) Kahan, J. S.; Kahan, F. M.; Goegelman, R.; Currie, S. A.; Jackson, M.; Stapley, E. O.; Miller, T. W.; Miller, A. K.; Hendlin, D.; Mochales, S.; Hernandez, S.; Woodruff, H. B.; Birnbaum, J. *J. Antibiot.* (*Tokyo*) **1979**, *32*, 1–12.

(4) Clissold, S. P.; Todd, P. A.; Campoli Richards, D. M. *Drugs* **1987**, *33*, 183–241.

(5) Kattan, J. N.; Villegas, M. V.; Quinn, J. P. *Clin. Microbiol. Infect.* **2008**, *14*, 1102–1111.

(6) Livermore, D.; Mushtaq, S.; Warner, M. *J. Antimicrob. Chemother.* **2005**, *55*, 306–311.

(7) Hanessian, S.; Desilets, D.; Bennani, Y. L. *J. Org. Chem.* **1990**, *55*, 3098–3103.

(8) Tatsuta, K.; Takahashi, M.; Tanaka, N.; Chikauchi, K. *J. Antibiot.* **2000**, *53*, 1231–1234.

(9) Woźnica, M.; Kowalska, P.; Łysek, R.; Masnyk, M.; Górecki, M.; Kwit, M.; Furche, F.; Frelek, J. *Curr. Org. Chem.* **2010**, *14*, 1022–1036.

(10) (a) Keith, D. D.; Tengi, J.; Rossman, P.; Todaro, L.; Weigele, M. *Tetrahedron* **1983**, *39*, 2445–2458. (b) Nangia, A.; Desiraju, G. R. *J. Mol. Struct.* **1999**, *47*, 65–79. (c) Cohen, N. C. *J. Med. Chem.* **1983**, *26*, 259–264. (d) Diaz, N.; Suarez, D.; Sordo, T. L. *J. Comput. Chem.* **2003**, *24*, 1864–1873.

(11) Kinugasa, M.; Hashimoto, S. *J. Chem. Soc., Chem. Commun.* **1972**, 466–467.

(12) (a) Stecko, S.; Mames, A.; Furman, B.; Chmielewski, M. *J. Org. Chem.* **2008**, *73*, 7402–7404. (b) Stecko, S.; Mames, A.; Furman, B.; Chmielewski, M. *J. Org. Chem.* **2009**, *74*, 3094–3100.

(13) Alcaide, B.; Benito, J.; Rodríguez-Campos, I.; Rodríguez-López, J.; Rodríguez-Vicente, A.; Sierra, M.; García-Granda, S.; Gutíerrez-Rodríguez, A. *Tetrahedron: Asymmetry* **1995**, *6*, 1055–1058.

SCHEME 2

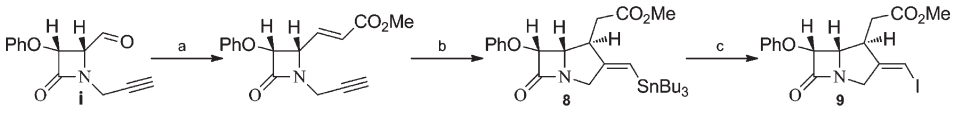

a: $Ph_3P{=}CH_2CO_2Me$; b: Bu_3SnH, AIBN; c: I_2, CH_2Cl_2, rt

SCHEME 3

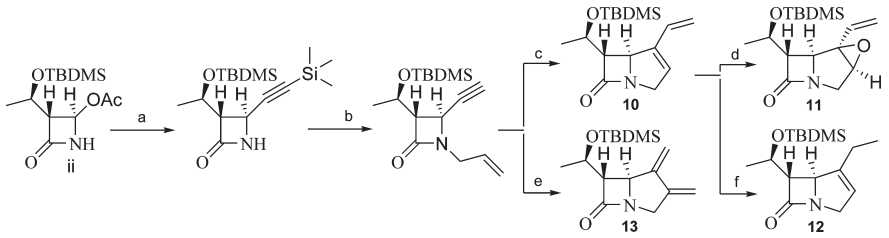

a: $CH{\equiv}CSiMe_3$, BuLi, THF, -78 °C; b: allyl bromide, NaH, DMF; c: Grubbs-Hoveyda second generation catalyst, CH_2Cl_2, 45 °C; d: air, rt.; e: $(Ph_3P)_2$, $Pd(OAc)_2$, benzene, 60 °C; f: H_2, Pd/C, C_2H_5OH.

TABLE 1. UV and ECD Data of β-Lactams 1−13 Recorded in Acetonitrile in the Range of 190−380 nm

compd	UV ε (λ_{max}); [$M^{-1}cm^{-1}$(nm)]			CD $\Delta\varepsilon$ (λ_{max}); [M^{-1} cm^{-1} (nm)]		
1	3970 (201)	420 (237)		+13.88 (203.0)	−15.13 (234.0)	
2	4500 (202)	670 (234)		+14.24 (202.0)	−17.95 (233.0)	
3	3700 (208)	680 (240)		+8.15 (204.5)	−10.91 (236.0)	
4	4300 (204)	560 (237)		−8.63 (204.0)	+15.67 (235.0)	
5	3900 (204)	500 (236)		+17.55 (203.5)	−20.25 (236.0)	
6	4100 (204)	490 (236)		−13.28 (204.0)	+17.72 (234.5)	
7	10600 (207)		420 (259)	+14.76 (207.0)	−17.52 (236.0)	*a*
8	19500 (218)		1200 (268)	−17.04 (225.0)	−7.97 (246.0^{sh})	+0.35 (277.0)
9	21400 (220)		1540 (268)	−23.05 (224.5)	−10.05 (240.0^{sh})	+0.71 (276.5)
10	12600 (224)	8800 (236^{sh})		−16.02 (218.0)[b]	+11.48 (245.0)	
11	10600 (196)	570 (230^{sh})		−35.43 (201.0)	+17.49 (231.5)	
12	6600 (201)	650 (240^{sh})		−28.78(201.0)	+17.02 (238.5)	
13	8100 (196)	6400 (246)		−12.03 (199.5)	+15.69 (234.0)	−1.48 (264.0)

[a] An absorption band of the phenyl substituent at C6 is hidden under the main ECD band at 236 nm. [b] An additional positive ECD band is observed at around 196 nm.

The synthetic route leading to compounds **10** and **11** is presented in Scheme 3. The key step in this synthesis was the ring-closing enyne metathesis (RCM) performed, in general, according to the known procedure.[14] The only difference was the use of the Grubbs−Hoveyda second-generation catalyst in place of Grubbs' second-generation catalyst, which enabled us to obtain the product almost quantitatively. Selective hydrogenation of compound **10** in the presence of Pd/C led to partially hydrogenated product **12**. Carbapenam **13** was obtained according to the literature procedure.[15] As a substrate in the synthesis of carbapenams **10**−**13** chiral Kaneko azetidinone **ii** was used.[16]

Interestingly, diene **10** underwent spontaneous oxidation by air oxygen to form epoxide **11** after 3 days standing at room temperature in a 70% yield. The absolute configuration at C3 was assigned on the basis of extended NMR experiments using the NOE technique.

2b. Experimental ECD Results. The UV and ECD data of carbapenams **1**−**13** are collected in Table 1. On the basis of these data, the investigated compounds can be divided into two groups considering the absolute configuration at the C5 carbon atom (5*R* or 5*S*) and the presence of an additional chromophore interfering with the amide absorption bands. In the group comprising compounds **7**−**10** and **13**, besides the amide chromophore, additional chromophoric groups such as the phenyl, phenoxyl, or diene system are present. All of them absorb strongly in the same spectral region as the amide chromophore.

In context of the selected series of compounds **1**−**13**, it became obvious that the direct application of *CIP* rules for the stereochemistry designation results in a somewhat confusing situation due to the need to change the *R* and *S* descriptors depending on the identity of substituent at the C4 position. This is particularly evident in the case of compounds **5**−**7** and **10**−**13** where, because of the application of *CIP* priority rules, the identity of substituent at C4 causes the change of absolute configuration descriptors from *S* to *R* and vice versa without any change of the actual stereochemical arrangement at the C5 carbon atom. Therefore, for the carbapenams studied here we decided to use the D and L nomenclature system, as defined in Figure 1.

As shown in Table 1 and Figure 2, two main bands are present in the ECD spectra of investigated compounds in the spectral range 200−250 nm. For the purpose of our studies, the band occurring at around 240 nm is of a particular

(14) (a) Desroy, N.; Robert-Peillard, F.; Toueg, J.; Duboc, R.; Henaut, C.; Rager, M.-N.; Savignac, M.; Genet, J.-P. *Eur. J. Org. Chem.* **2004**, 4840–4849. (b) Duboc, R.; Henaut, C.; Savignac, M.; Genet, J.-P.; Bhatnagar, N. *Tetrahedron Lett.* **2001**, *42*, 2461–2464.

(15) Trost, B. M.; Chen, S.-F. *J. Am. Chem. Soc.* **1986**, *108*, 6053–6054.

(16) (a) Sada, I.; Kan, K.; Ueyama, N.; Matsumoto, S.; Ohashi, T.; Watanabe, K. Eur. Pat. Appl. EP 280962 A1, 1988. (b) Yamada, Y.; Kaneko, A. JP 9016042, 1990.

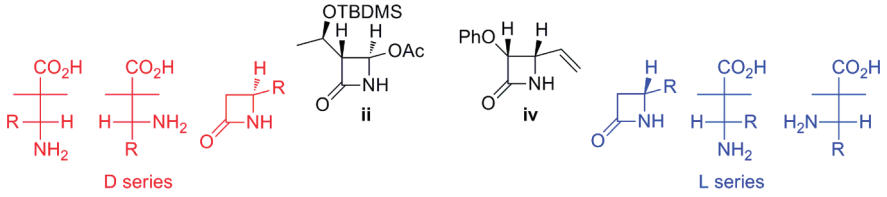

FIGURE 1. Definition of the D- and L-series.

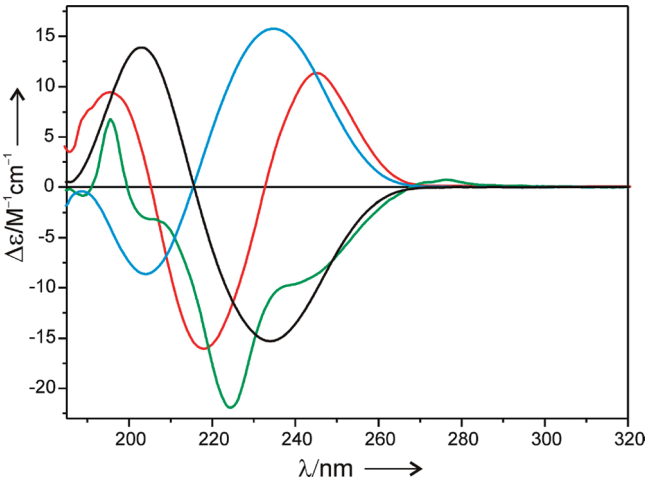

FIGURE 2. CD spectra of carbapenams **1** (black line), **4** (blue line), **9** (green line), and **10** (red line) recorded in acetonitrile.

interest because it is the subject of the helicity rule. Regarding this ECD band, the investigated compounds fall into two different classes. In the first class, consisting of compounds **1**−**3**, **5**, and **7**−**9** the sign of the 240 nm CD band is negative, whereas in the second class, represented by compounds **4**, **6**, **10**−**13**, its sign is positive (Table 1).

According to the helicity rule, compounds with a positive 240 nm CE should belong to the D-series, whereas the negative sign of this CE indicates the membership of the L-series.[2,9] This prediction has been confirmed by X-ray analysis for carbapenam **7**.[12a] In addition, the X-ray data of **7** demonstrate the pyramidality of the β-lactam nitrogen atom as evidenced by the distance 43.3 pm of the nitrogen atom from the least-squares plane containing C2, C5, and C7 carbon atoms (see Table 2 in section 2c). The sign of the O=C−N−C2 and O=C−N−C5 torsional angles for **7** is positive, and accordingly, the sign of the long-wavelength CE at 236 nm is negative (Table 1). The signs are exactly what one would expect to see when applying the helicity rule. Thus, it can be concluded that for carbapenam **7** the helicity rule works well and correlates the sign of the O=C−N−C2 and O=C−N−C5 torsional angles with the sign of the long-wavelength CD band at around 240 nm. As can also be seen from Table 1, the carbapenams **1**−**7**, **11**, and **12** also perfectly conform to this regularity.

A more complex situation occurs in carbapenams **8**−**10** and **13** due to the presence of groups strongly interfering with the amide chromophore. The phenoxy substituent at C6 in carbapenams **8** and **9** absorbs at similar wavelengths as the amide chromophore, which greatly complicates the ECD spectra. In the case of carbapenams **10** and **13**, the presence of a highly absorbing and strongly interfering diene system causes further complications. On account of this the shape of the ECD curves markedly differs from the shape of the curves of remaining carbapenams (Table 1, Figure 2).

2c. Calculated ECD Spectra. In order to ascertain whether the helicity rule correctly predicts the absolute stereochemistry for investigated carbapenams, the TDDFT calculations using the B3LYP/TZVP method were performed for selected compounds, namely **1**, **2**, **6**, **7**, **10**, and **13**. The results should give more insight into the conformational and chiroptical behavior of compounds **1**−**13**.

First, we sought the validation of our calculation methodology by direct comparison of the geometry-related data obtained from the X-ray studies and from the molecular modeling of carbapenam **7**. The results demonstrate a good conformity between the calculated and the solid-state values (Table 2) and prove the correctness of the calculation methodology used for this group of compounds. Thus, for the remaining carbapenams, which do not form crystals suitable for the X-ray analysis, the same TDDFT calculation methodology was applied. The selected structural data for lowest energy conformers of compound **1**, **2**, **6**, **7**, **10**, and **13** are collected in Table 2.

The bicyclic system of carbapenams is relatively rigid, and its conformational lability is largely restricted to the side-chain substituent at the C6 carbon atom. Its relatively unrestricted mobility is evident considering the results of conformational search for individual carbapenams. In the case of carbapenam **1**, nine conformers in the energy range of 2.4 kcal/mol were found (Table 3). In respect to the five-membered ring conformation space, however, only two conformers are found. In the first one, populated in the conformational equilibrium over 75%, the five-membered ring is in an envelope conformation with C4 carbon atom below the average plane passing through the ring. In the second conformer, the five-membered ring adopts a half-chair conformation with C2 and C3 carbon atoms located above and below the ring plane, respectively (Figure 3). Beyond these two, the other individual conformers show differences in the substituent at C6 carbon atom which demonstrates its relatively substantial flexibility (Table 3, Figure 3).

The O8−C7−N1−C2 and O8−C7−N1−C5 torsion angles for all conformers is calculated to be positive. In simulated ECD spectra the sign of the lowest energy excitations is negative for all conformers. The average ECD spectrum shows very close agreement between experiment and theory thus providing evidence that these conformers are present in solution under given conditions (Figure 4). The negative CE at around 240 nm is in accordance with both the helicity rule and the calculations.

The substitution of the five-membered ring with a large group upsets the balance of strain in the ring and makes one of the symmetrical ring conformations the lowest in energy.[17] This

(17) Eliel, L. L.; Wilen, S. H. *Stereochemistry of Organic Compounds*; J. Wiley & Sons, Inc.: New York, 1994; pp 758−761.

TABLE 2. Selected Torsional Angles (deg) and Pyramid Height for the N-Atom (pm) Determined by X-ray Diffraction and Calculated by B3LYP/TZVP Method

compd	conf. series	240 nm obs	CE sign pred		6−7−1−5	8−7−1−2	8−7−1−5	6−7−1−2	pyr height
1	L	(−)	(−)	calcd	−10.0	+43.1	+166.9	−133.75	40.8
2	L	(−)	(−)	calcd	−10.1	+57.4	+166.3	−133.3	41.4
6	D	(+)	(+)	calcd	+9.8	−42.3	−167.3	+134.66	39.7
7	L	(−)	(−)	X-ray	−11.0	+45.0	+166.9	−132.8	43.3
				calcd	−9.4	+43.2	+168.3	−134.4	39.7
10	D	(+)	(+)	calcd	+6.8	−53.1	−170.1	+123.8	49.0
13	D	(+)	(+)	calcd	+6.6	−48.6	−170.5	+128.46	42.9

TABLE 3. Selected Torsional Angles (deg), ΔE (kcal/mol), Conformer (Conf) Distribution (D) (%), and Pyramidal Height (Pyr) for the N-Atom (pm) Determined by the B3LYP/TZVP Method of Compound 1 Conformers

conf	ΔE	D	8−7−1−5	8−7−1−2	1−2−3−4	2−3−4−5	3−4−5−1	4−5−1−2	5−1−2−3	pyr
1	0.00	37.16	166.93	43.14	−23.00	+36.50	−34.73	+21.98	+0.60	40.8
2	0.32	21.65	167.06	43.46	−24.15	+37.35	−34.91	+21.40	+1.67	41.0
3	0.53	15.18	166.82	42.95	−23.23	+36.72	−34.82	+21.92	+0.78	40.6
4	0.74	10.65	168.66	49.71	+32.08	−24.31	+7.05	+14.15	−29.13	46.2
5	0.99	6.98	168.59	49.57	+31.99	−24.41	+7.26	+13.89	−28.92	46.2
6	1.29	4.21	168.94	50.00	+32.40	25.03	+7.88	+13.49	−28.93	46.2
7	1.52	2.85	167.84	43.56	−24.08	+37.33	−34.97	+21.53	+1.54	40.2
8	2.37	0.68	169.97	50.53	+32.09	−25.20	+8.48	+12.61	−28.14	45.7
9	2.41	0.63	169.49	20.21	+32.30	−25.49	+8.71	+12.52	−28.24	46.0

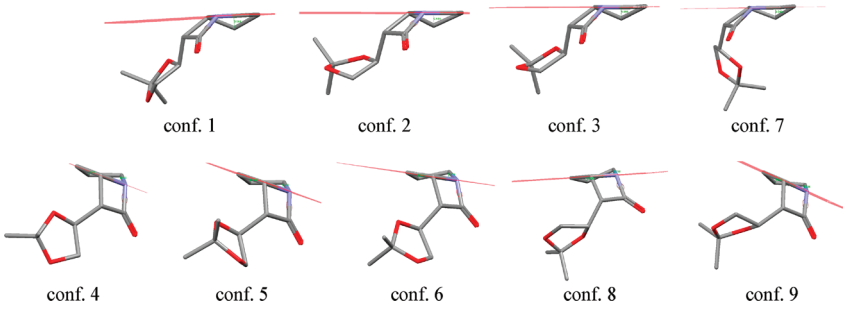

FIGURE 3. Structures of the low energy conformers of **1** calculated at the B3LYP/TZVP theory level: upper panel, envelope conformers; lower panel, half-chair conformers.

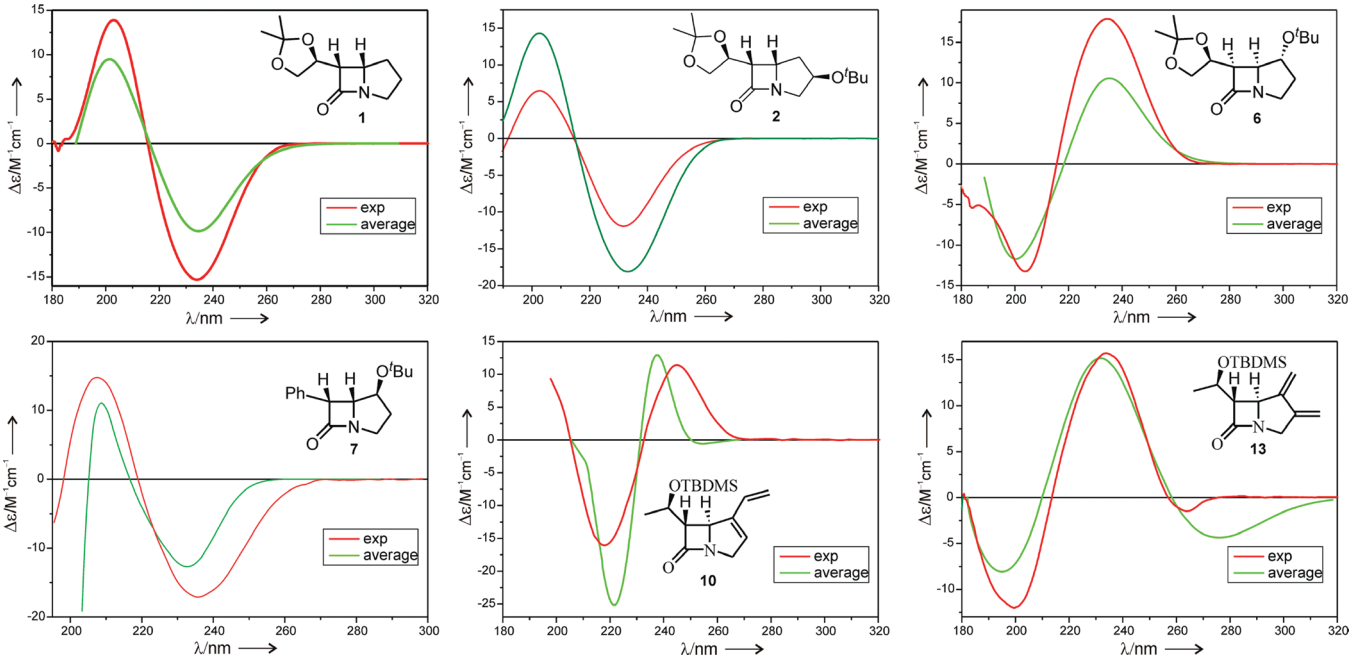

FIGURE 4. Experimental ECD spectra in acetonitrile solution (red lines) and calculated at B3LYP/TZVP theory level average CD spectra (green lines) for carbapenams **1**, **2**, **6**, **7**, **10**, and **13**.

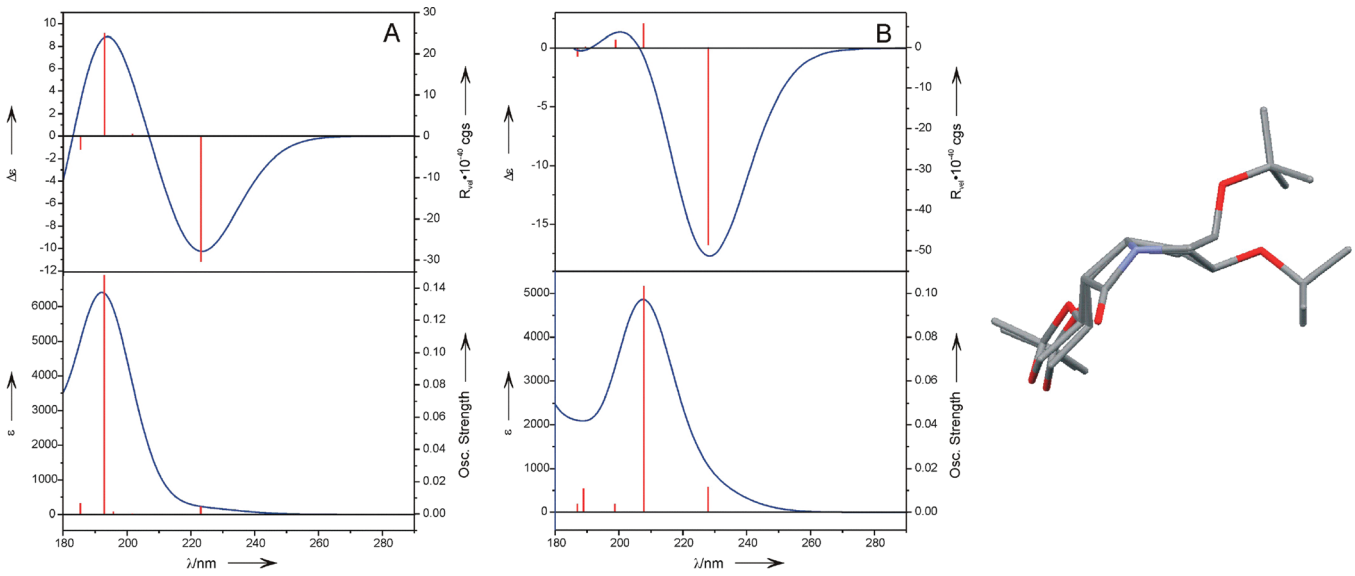

FIGURE 5. Left: simulated ECD and UV spectra of the lowest (A) and next lowest (B) energy conformers of **2**. Right: an overlay of two main conformers of carbapenam **2**. Hydrogen atoms are omitted for clarity. ε is the molar decadic absorption coefficient, λ the wavelength, and R the computed rotatory strength.

is indeed observed for the examined *tert*-butoxy-substituted carbapenams. And so, in the case of carbapenam **2** substituted with a *tert*-butoxy group at the C3 carbon atom, the number of conformers in conformational equilibrium is reduced considerably compared with unsubstituted compound **1**. In fact, two main conformers populated in over 90% were found in the energy range of 1 kcal/mol. In respect to the five-membered ring conformation space, the lowest energy conformer, distributed in conformational equilibrium in over 75%, adopts an envelope conformation with C4 carbon atom below the average plane passing through the ring. In the second conformer, higher in energy by 0.88 kcal/mol, the five-membered ring also occurs in an envelope conformation but this time with the C2 carbon atom above the ring plane, as shown in Figure 5. The simulated average spectrum is in an excellent agreement with the experimental one (Figure 4) confirming both the absolute configuration and conformation of this carbapenam.

For carbapenam **7** with a *tert*-butoxy substituent located at C4, three conformers were found within the energy range of 2 kcal/mol. The lowest energy conformer, distributed in over 55%, possesses the envelope conformation with C4 carbon atom below the ring plane. The second conformer, higher in energy by 0.26 kcal/mol and distributed in ca. 37%, occurs also in an envelope conformation but with the C2 carbon atom above the ring plane. Regarding the five-membered ring conformation, the highest energy conformer (higher in energy by 1.44 kcal/mol and distributed in 5%) exists in the same conformation as the lowest energy one. These minor conformational differences caused by the substituent at C4 and side-chain flexibility are reflected in the simulated ECD curves for each of the conformers (Figure 6). Nevertheless, the agreement between the experimental and simulated average ECD curves is very satisfactory, confirming experimentally and theoretically the three-dimensional structure of **7** (Figure 4).

For carbapenam **6** in the energy range of 3 kcal/mol seven conformers were found. However, only two of those are

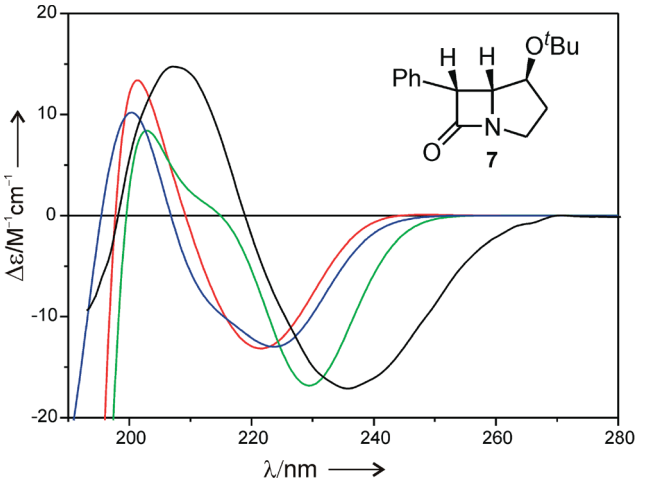

FIGURE 6. Experimental ECD spectrum in acetonitrile solution of carbapenam **7** (black line) and calculated at the B3LYP/TZVP theory level spectra of its lowest energy conformer (red line), medium energy conformer (green line), and highest energy conformer (blue line).

important, considering the conformational changes of five-membered ring. Similarly to carbapenam **1**, significantly populated conformers (over 70%) adopt an envelope conformation whereas the remaining ones are in a half-chair conformation (see the Supporting Information). In all conformers, the *tert*-butoxy substituent occupies an equatorial position. In this case again, the average ECD spectrum is in an excellent agreement with experiment and confirms the absolute configuration and conformation of **6** (Figure 4).

In the case of compounds **10** and **13**, both bearing a diene unit in the molecule, the number of calculated conformers is four and three, respectively. In all these conformers the five-membered ring is nearly planar with nitrogen atom slightly deviated from the plane formed by four carbon

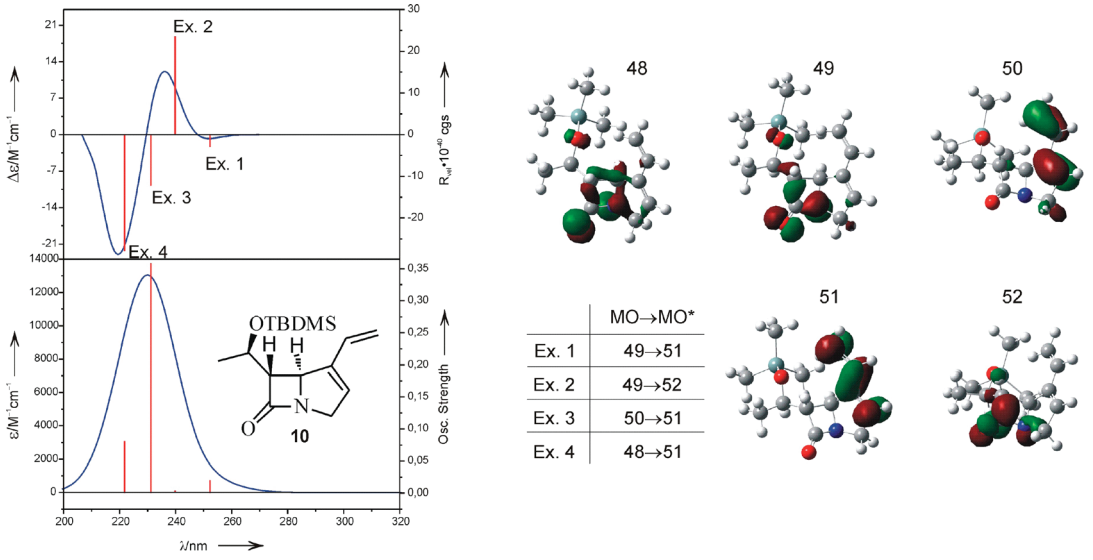

FIGURE 7. Left: simulated ECD and UV spectra of lowest energy conformer of carbapenam **10**. Right: dominant contributions of MOs of particular excitations of carbapenam **10** lowest energy conformer.

atoms. Similarly to the compounds discussed earlier the conformational differences in **10** and **13** are limited mostly to the differences in side chain conformations. In all conformers calculated for **10** and **13** the O8−C7−N1−C2 and O8−C7−N1−C5 torsion angles are negative and the sign of ECD band around 240 nm is calculated to be positive in agreement with experiment. On the basis of calculation results for compound **10** presented in Figure 7, it can be stated that this band is an admixture of the amide n→π* transition and of the diene π→π* transition occurring at 240 and 252 nm, respectively (MO49→MO*52 and MO49→MO*51, respectively). To simplify and speed up the calculations, as well as shorten the computational time, calculations of compound **10** were conducted only for the first four electronic transitions. Unfortunately, these parameters seem to be insufficient to determine the π−π* amide transition in the simulated ECD spectrum, i.e. transition MO48→MO*52. This simplification, however, did not affect the result of calculation in the energy range of n−π* amide transition (MO49→MO*52) which is crucial in terms of helicity rule.

Regardless of the complexity of the electronic transitions within the band at 240 nm, the positive sign of its component related to the amide n→π* excitation and decisive in terms of the helicity rule, is in accord with the rule. In addition, the agreement between the experimental and Boltzmann-averaged ECD spectra is very accurate and confirms both absolute configuration and conformation of carbapenams **10** and **13** (Figure 4).

3. Conclusions

The relationship between the molecular structure and the chiroptical properties of carbapenams **1**−**13** was investigated by X-ray diffraction analysis, electronic circular dichroism spectroscopy, and time-dependent density functional theory. The computed O8−C7−N1−C2 and O8−C7−N1−C5 torsion angles for compounds **1**, **6**−**8**, **10**, and **12** provide corroborating evidence for the nonplanarity of amide chromophore. The band at 240 nm has mainly the character of an amide n(O)→π* transition. Its positive or negative sign, depending upon the D- or L-configuration, respectively, is predicted by both the helicity rule and the TDDFT calculations. Thus, we can conclude that the helicity rule is valid for the investigated carbapenams.

The simulated spectra resemble smoothed experimental spectra and represent the theoretical and experimental estimates of rotational strength faithfully and equivalently. The very good agreement between the simulated and the experimental ECD spectra allows one to assign the absolute configuration at the ring junction in carbapenams **1**−**13** with satisfactory accuracy. The study demonstrated a high sensitivity of the ECD spectra for even the smallest conformational differences caused by substitution of the five-membered ring and side-chain flexibility. The presence of an additional, interfering chromophore in the molecule complicates interpretation of results. Nevertheless, it is demonstrated that even in such cases the determination of stereostructure of carbapenams is possible with a high degree of confidence on the basis of combined experimental and theoretical studies.

Recapitulating, ECD spectroscopy as a highly sensitive probe for elucidation of the three-dimensional molecular structure can be successfully utilized to the configurational and conformational analysis of two- and multifunctional carbapenams with one or more stereogenic centers. However, we strongly recommend supporting experimental data by computational results. Such an approach allows one to read and understand the complex information contained in electronic CD spectra.

4. Experimental Section

The UV spectra were measured using a Cary 100 spectrophotometer in acetonitrile solutions. The CD spectra, recorded on a JASCO J-815 spectropolarimeter as mdeg spectra, were converted into $\Delta\varepsilon_{max}$ (M^{-1} cm^{-1})/λ (nm) units. Solvents for circular dichroism measurements were spectroscopic grade. The solutions were examined between 185 and 400 nm at room temperature in cells with the path length of 0.05−1 cm and concentrations in the range of 0.3×10^{-4} to 1.0×10^{-3} mol·dm^{-3}.

Preparation of New Model Compounds. 8-[1-(*tert*-Butyldimethylsilanyloxy)ethyl]-2-vinyl-3-oxa-6-azatricyclo[4.2.0.0^{2,4}]-octan-7-one (11). Compound **10** (40 mg, 0.136 mmol) was dissolved in dry dichloromethane (10 mL), and the solution was kept aside at room temperature in the air atmosphere until the substrate disappeared (ca. 3 days). The mixture was chromatographed on silica gel (10% AcOEt in Hex), and the solvent was removed. Product **11** was obtained in 67% yield (28 mg) as colorless crystals (fine needles): $[\alpha]_D$ −0.45 (*c* 0.62, CH_2Cl_2); ^{1}H NMR (500 MHz, $CDCl_3$) δ 0.077 (s, 3H), 0.082 (s, 3H), 0.89 (s, 9H), 1.23 (d, J = 6.2 Hz, 3H), 3.00 (dd, J = 13.3, 0.6 Hz, 1H), 3.11 (ddd, J = 5.3, 1.9, 1.0 Hz, 1H), 3.66 (t, J = 0.8 Hz, 1H), 3.85 (d, J = 13.3 Hz, 1H), 3.88 (d, J = 1.9 Hz, 1H), 4.21 (p, J = 6.2 Hz, 1H), 5.42 (dd, J = 10.9 Hz, 1.0 Hz, 1H), 5.58 (dd, J = 17.6 Hz, 1.0 Hz, 1H), 5.90 (dd, J = 17.6 Hz, 10.9 Hz, 1H); ^{13}C NMR (125 MHz, $CDCl_3$) δ −4.84, −4.39, 17.98, 22.90, 25.76 (3C), 48.57, 53.70, 58.85, 65.35, 65.50, 69,08, 120.32, 130.82, 177.65; HR MS (ESI) calcd for $[M + Na]^+C_{16}H_{27}NO_3NaSi$ 332.1652, found 332.1656; IR (film) ν/cm^{-1} 1771, 1472, 1253, 1103, 837, 776.

6-[1-(*tert*-Butyldimethylsilanyloxy)ethyl]-4-ethyl-1-azabicyclo-[3.2.0]hept-3-en-7-one (12). Compound **10** (90 mg, 0.307 mmol), ethanol (10 mL), and 10% Pd on charcoal (9 mg) were placed in a flask equipped with a magnetic bar, and the flask was attached to the apparatus for hydrogenation. The flask was filled with hydrogen, and the magnetic stirrer was turned on. The vigorous stirrinng was continued until the initial fast hydrogen consumption significantly slowed down. The mixture was then filtered through a pad of Celite, the ethanol was evaporated, and the residue was chromatographed on silica gel (10% AcOEt in Hex). Product **12** was isolated as a colorless oil in 30% yield (31 mg): $[\alpha]_D$ +47.08 (*c* 0.67, CH_2Cl_2); ^{1}H NMR (500 MHz, $CDCl_3$) δ 0.088 (s, 3H), 0.089 (s, 3H), 0.90 (s, 9H), 1.13 (t, J = 7.4 Hz, 3H), 1.25 (d, J = 6.2 Hz, 3H), 2.12−2.19 (m, 2H), 2.91 (ddd, J = 6.2, 2.5, 0.6 Hz, 1H), 3.49−3.55 (m, 1H), 4.18−4.22 (m, 2H), 4.28−4.33 (m,1H), 5.50 (bs, 1H); ^{13}C NMR (125 MHz, $CDCl_3$) δ −4.85, −4.31, 12.28, 17.95, 20.99, 22.72, 25.73 (3C), 53.26, 62.85, 65.92, 66.15, 124.12, 145.24, 180.74; HR MS (ESI) calcd for $[M + Na]^+$ $C_{16}H_{29}NO_2NaSi$ 318.1860, found 318.1865; IR (film) ν/cm^{-1} 1770, 1463, 1258, 1140, 836, 776.

Calculations. In our computations, all calculations have been performed using the Gaussian program package.[18] The CD spectra were simulated by overlapping Gaussian functions for each transition according to the procedure described by Grimme.[19] Conformational analyses were performed using HyperChem software[20] and the MM2 force field. Conformers found with the use of molecular mechanics were optimized using the B3LYP hybrid functional, TZVP basis set, and the PCM solvent model for acetonitrile. Then, for the conformers with relative energies ranging from 0 to 3 kcal/mol the population percentages were calculated using ΔE applying Boltzmann statistics and T = 298 K.

For all conformers (excluding those with the population percentage lower than 1%), the oscillator and rotathory strengths were calculated at the TD-B3LYP/TZVP theory levels using the PCM solvent model for acetonitrile. The calculated spectra were Boltzmann averaged according to the population percentages of individual conformers. In the case of all conformers, the calculated CD and UV spectra were red-shifted by ca. 10 nm in relation to the experimental ones.

Acknowledgment. This work was supported by the Polish State Committee for Scientific Research (KBN) (Grant Nos. N N204 123507 and N N204 092935). We acknowledge a grant for computational time at the Interdisciplinary Centre for Mathematical and Computational Modelling (ICM) of University of Warsaw, Poland. The authors are grateful to Professor S. Grimme and his co-worker H. Kruse for calculating of compound **10** and helpful comments.

Supporting Information Available: Details of general experimental methods, ^{1}H and ^{13}C NMR, MS, IR spectra for reported compounds, calculated structures of conformers of **1**, **6**−**8**, **10**, and **12**, all calculated UV and CD spectra, total energies, relative energies, and Cartesian coordinates for all optimized structures used in this work. This material is available free of charge via the Internet at http://pubs.acs.org.

(18) Frisch, M. J.; Trucks, G. W.; Schlegel, H. B.; Scuseria, G. E.; Robb, M. A.; Cheeseman, J. R.; Zakrzewski, V. G.; Montgomery, J. A., Jr.; Stratmann, R. E. B.; J. C.;, Dapprich, S.; Millam, J. M.; Daniels, A. D.; Kudin, K. N.; Strain, M. C.; Farkas, O.; Tomasi, J.; Barone, V.; Cossi, M.; Cammi, R.; Mennucci, B.; Pomelli, C.; Adamo, C.; Clifford, S.; Ochterski, J.; Petersson, G. A.; Ayala, P. Y.; Cui, Q.; Morokuma, K.; Salvador, P.; Dannenberg, J. J.; Malick, D. K.; Rabuck, A. D.; Raghavachari, K.; Foresman, J. B.; Cioslowski, J.; Ortiz, J. V.; Baboul, A. G.; Stefanov, B. B.; Liu, G.; Liashenko, A.; Piskorz, P.; Komaromi, I.; Gomperts, R.; Martin, R. L.; Fox, D. J.; Keith, T.; M. A. Al-Laham, Peng, C. Y.; Nanayakkara, A.; Challacombe-Gonzalez, C.; M. Head-Gordon, Replogle, E. S.; Pople, J. A. Gaussian 03; Gaussian, Inc.; Pittsburgh, PA, 2001.

(19) Diedrich, C.; Grimme, S. *J. Phys. Chem. A* **2003**, *107*, 2524–2539.

(20) HyperChem(TM) Professional 8.0; Hypercube, Inc.: Gainesville, FL.